

Cite this: *Soft Matter*, 2011, **7**, 6811

www.rsc.org/softmatter

## Micro-patterns of reduced graphene oxide (RG-O) platelets crafted by a self-assembled template†

Soon Woo Kwon,<sup>‡a</sup> Tae Young Kim,<sup>‡b</sup> Yena Kim,<sup>a</sup> Myunghwan Byun,<sup>c</sup> Zhiqun Lin,<sup>cd</sup> Kwang S. Suh,<sup>b</sup> Dae Ho Yoon<sup>\*a</sup> and Woo Seok Yang<sup>\*e</sup>

Received 26th April 2011, Accepted 16th June 2011

DOI: 10.1039/c1sm05761h

**Highly ordered reduced graphene oxide (RG-O) micro-patterns were crafted by an efficient method capitalizing on the self-assembled polymer template. Central to this strategy is to fabricate the polymer template over a large area via controlled evaporative self-assembly (CESA), and treat the templated glass substrate with the O<sub>2</sub> plasma to render the favorable interaction between the RG-O platelets and the substrate, thereby yielding well-defined microscopic RG-O patterns on the large scale.**

Owing to its outstanding properties, such as high optical transparency, flexibility, and excellent electrical and thermal conductivities, graphene, a single atomic layer of carbon arranged in a honeycomb structure, has been the subject of intense scientific and industrial research.<sup>1–6</sup> More importantly, graphene can be readily produced in a wide range of processable forms in large quantities using simple chemical processes.<sup>7–10</sup> As such, graphene and its chemically modified forms are promising carbon nanomaterials for various technological applications, including field-effect devices, chemical sensors, energy conversion and storage devices, electrocatalysis, *etc.*<sup>1–10</sup>

For the fabrication of graphene-based devices, it is highly desirable to control the assembly of graphene-based nanomaterials into a specific architecture. To this end, the previous methods mainly relied on top-down lithography techniques to create the surface patterns on the substrate.<sup>11,12</sup> However, these methods are limited by the high cost and low throughput, and thus there is a need to develop alternative techniques to pattern graphene-based materials. In

parallel with top-down nanotechnology, significant advances in the bottom-up approaches based on self-assembly have made it possible to produce patterns with long-range order.<sup>13–16</sup> Hierarchical structures can be spontaneously formed from an evaporating solution containing nonvolatile solutes *via* the control of the interaction between the solute and the substrate. Among them, recently controlled evaporation-induced self-assembly in a restricted geometry has been recognized as a simple yet robust nonlithography route to producing intriguing patterns with unprecedented regularity composed of polymers, nanocrystals, carbon nanotubes, *etc.*<sup>17–32</sup> In this context, there has been considerable interest in capitalizing on graphene-based materials in solution to assemble them into complex architectures with unexplored functionalities. Despite the previous efforts on the arrangement of graphene-based platelets that yields papers, thin films, and other constructs,<sup>33–35</sup> the assembly of two-dimensional (2D) graphene sheets into complex architecture has not yet been realized.

Herein, we report on the crafting of reduced graphene oxide (RG-O) micropatterns over large surface areas using the self-assembled polymer template in a simple, cost-effective, and scalable manner. The highly ordered poly(methylmethacrylate) (PMMA) stripes were first obtained by controlled evaporative self-assembly (CESA) of the PMMA toluene solution in a cylinder-on-flat geometry. Subsequently, the stripes were treated with the O<sub>2</sub> plasma and exploited as a chemically patterned surface to direct the assembly of RG-O microstructures by allowing a drop of poly(ionic liquid)-modified RG-O (PIL:RG-O) suspension cast on the surface of the PMMA template to dry, followed by the removal of PMMA with selective solvent. The combination of spontaneous *controlled evaporative self-assembly (CESA)* and subsequent *directed assembly* offers a new means of patterning RG-O at the microscopic scale. This method is fast and cost-effective, dispensing with the need for multistage lithography and externally applied forces.

A homogeneous suspension of RG-O sheets was prepared by chemical reduction of an aqueous graphene oxide (G-O) suspension using hydrazine monohydrate at 90 °C for 1 h in the presence of poly(ionic liquids) (PILs) as shown in Fig. 1a (see *Experimental section*). It has been demonstrated that PILs, specifically poly(1-vinyl-3-ethylimidazolium) bromide, are easily physisorbed onto the RG-O surface *via* electrostatic interaction or cation– $\pi$  interaction, and can stabilize the RG-O sheets in the aqueous suspension.<sup>36</sup> While the oxygen-rich functional groups on G-O are generally negatively charged,<sup>7–10</sup> RG-O

<sup>a</sup>School of Advanced Materials Science and Engineering, Sungkyunkwan University, Suwon, 440-746, Republic of Korea. E-mail: dhyoon@skku.edu; Fax: +82-31-290-7371; Tel: +82-31-290-7388

<sup>b</sup>Department of Materials Science and Engineering, Korea University, Seoul, 136-713, Republic of Korea

<sup>c</sup>Department of Materials Science and Engineering, Iowa State University, Ames, IA, 50011, USA

<sup>d</sup>School of Materials Science and Engineering, Georgia Institute of Technology, Atlanta, GA, 30332, USA

<sup>e</sup>Electronic Materials and Device Research Center, Korea Electronics Technology Institute, Seongnam, 463-816, Republic of Korea. E-mail: wsyang@keti.re.kr; Fax: +82-31-789-7249; Tel: +82-31-789-7256

† Electronic supplementary information (ESI) available: AFM and TGA data for G-O and PIL:RG-O materials. Additional data for the controlled pattern formation. See DOI: 10.1039/c1sm05761h

‡ These authors equally contributed to this work.

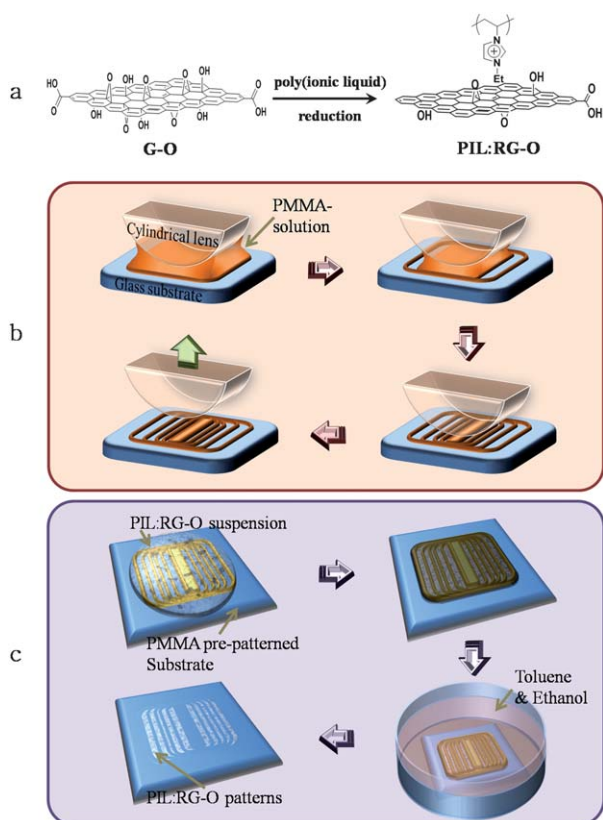


**Fig. 1** Schematic illustrations of (a) modification of reduced graphene oxide (RG-O) with poly(ionic liquid) (PIL), (b) formation of poly(methyl methacrylate) (PMMA) template on the glass substrate *via* the CESA process in a cylinder-on-flat geometry (*i.e.*, a cylindrical lens situated on the glass substrate), and (c) deposition of PIL:RG-O platelets on the PMMA templated glass substrate followed by the subsequent removal of PMMA.

sheets modified with PIL molecules are found to have positively charged surfaces, as evidenced by the surface charge measurements. In contrast to the  $\zeta$  potential value for the aqueous suspension of G-O platelets ( $-28$  mV), the value of the  $\zeta$  potential from the PIL-modified RG-O suspensions in water was  $37.3$  mV. The average thickness of the PIL:RG-O sheet was  $1.9$  nm.<sup>36</sup> It is noteworthy that the use of these PIL-modified RG-O (PIL:RG-O) materials is crucial to ensure the formation of RG-O micropatterns when cast onto the self-assembled polymer template as will be discussed later.

The highly ordered concentric rectangular PMMA stripes used as the template to guide the assembly of RG-O were prepared by controlled evaporative self-assembly (CESA) of the PMMA toluene solution ( $c = 0.8$  mg mL<sup>-1</sup>) in the cylinder-on-flat geometry composed of a cylindrical lens on the glass substrate as illustrated in Fig. 1b (see *Experimental section*). The PMMA toluene solution was trapped in this confined geometry, forming a capillary-held solution (first panel in Fig. 1b). The evaporation of toluene led to an outward flow of PMMA to the edge of the capillary to pin the contact line, forming a coffee ring-like deposit (*i.e.*, “stick”; second panel in Fig. 1b).<sup>37,38</sup> During the deposition of PMMA, the initial contact angle of the PMMA solution gradually decreased due to the continuous evaporative loss of toluene, causing an increase in the depinning force.<sup>28</sup> When the depinning force became larger than

the pinning force, the contact line became unstable and jumped (*i.e.*, “slip”) to the next position inward where it would be pinned again later on.<sup>28</sup> These repeated pinning and depinning cycles (*i.e.*, “stick–slip” motion) of three phase contact line yielded concentric rectangular shaped patterns globally governed by the shape of cylindrical lens used,<sup>28</sup> progressing to the cylindrical lens/glass substrate contact center (referred to “cylinder/glass” thereafter). Locally, the patterns appeared as parallel stripes (Fig. 2). Notably, the whole CESA process took only less than 30 min to complete. In contrast to the stripes formed at the outer region where the contact lines were far away from the cylinder/glass contact center (*i.e.*, at the beginning of the evaporation process) (Fig. 2b), the stripes obtained at the inner region (*i.e.*, at the late stage of the evaporative self-assembly process) composed of rather aggregated PMMA (Fig. 2c), which may result from less PMMA available to form a complete stripe.

The dimension of PMMA patterns was characterized by optical microscopy (OM) and atomic force microscopy (AFM). The width of PMMA stripes,  $w$ , and the average spacing between adjacent stripes,  $\lambda$ , were in the order of tens of micrometres. As evaporation progressed toward the cylinder/glass contact center,  $\lambda$  gradually

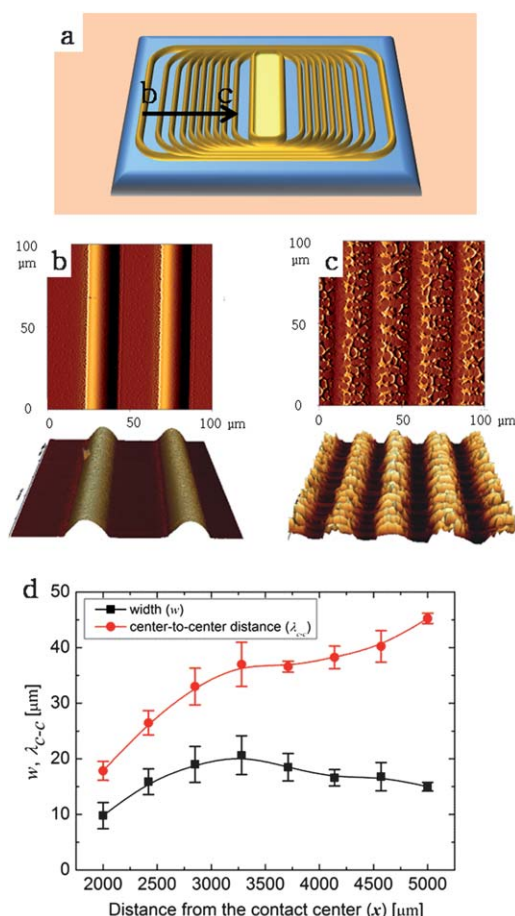


**Fig. 2** (a) Schematic of concentric rectangles of PMMA formed by CESA of the PMMA toluene solution in the cylinder-on-flat geometry, (b and c) AFM images of self-assembled PMMA patterns at the different locations of  $x$ , where  $x$  is the distance away from the cylinder/glass contact center. Scan size =  $100 \mu\text{m} \times 100 \mu\text{m}$ . (d) The width of PMMA pattern,  $w$ , and the average spacing between adjacent patterns,  $\lambda$ , as a function of  $x$ .

decreased from  $\lambda = 45.25 \pm 0.96 \mu\text{m}$  at  $x = 5000 \mu\text{m}$  to  $\lambda = 17.83 \pm 1.7 \mu\text{m}$  at  $x = 2000 \mu\text{m}$ , where  $x$  is the distance away from the cylinder/glass contact center. However,  $w$  of PMMA patterns slightly varied from  $w = 14.98 \pm 0.77 \mu\text{m}$  to  $w = 20.64 \pm 3.49 \mu\text{m}$  from  $x = 5000 \mu\text{m}$  to  $x = 3280 \mu\text{m}$ , respectively. As  $x$  further decreased (*i.e.*, from  $x = 3280$  to  $2000 \mu\text{m}$ , closer to the contact center),  $w$  gradually decreased from  $w = 20.64 \pm 3.49 \mu\text{m}$  to  $w = 9.78 \pm 2.36 \mu\text{m}$  (Fig. 2d). In general,  $w$  decreases as the evaporating front progressively approaches the contact center.<sup>27–29</sup> In the present study, however, the slight variation in  $w$  at  $x = 3280$ – $5000 \mu\text{m}$  can be attributed to the fact that toluene may begin to evaporate rapidly during this period of time, corresponding to the deposition at  $x = 3280$ – $5000 \mu\text{m}$ , before the loaded solution in the cylinder-on-flat geometry can stabilize to have controlled evaporation.

The stripe-like PMMA patterns were then exploited as the template to guide the assembly of RG-O platelets (*i.e.*, *directed assembly*). The PIL modification renders the production of a homogeneous, positively charged PIL:RG-O suspension in water. The placement of the PIL:RG-O suspension over the as-prepared PMMA micro-patterns initially resulted in poor wetting as evidenced in Fig. 3a. Therefore the PMMA template was then exposed to the O<sub>2</sub> plasma to enhance the hydrophilicity of the glass substrate. This led to a significant improvement in wetting of PIL:RG-O suspension and preferential adsorption of PIL:RG-O on the PMMA-patterned substrate (*i.e.*, the region that was not covered by PMMA; Fig. 3b), thereby facilitating the deposition of PIL:RG-O platelets in between the PMMA patterns as water evaporated. We believe such directed assembly was driven by the favorable electrostatic interaction between the positively charged PIL:RG-O platelets and the hydrophilic, negatively charged glass substrate that was uncovered by PMMA.

After selective removal of the PMMA template with toluene and ethanol, concentric PIL:RG-O rectangles were thus yielded. Locally, they appeared as stripes as shown in Fig. 4a and b. It is clearly evident that the dimension of microscopic PIL:RG-O patterns was commensurate with that of PMMA templates, and the size and shape of PIL:RG-O stripes were retained after the removal of PMMA (Fig. 4c). Also, the dimension of these patterns could be controlled by PMMA concentration in solution (see ESI†). The success of formation of RG-O platelet micropatterns templated by PMMA stripes was further confirmed by Raman spectroscopy measurements (Fig. 4d). The Raman spectrum of as-obtained PIL:RG-O patterns displayed a D-band at  $1350 \text{ cm}^{-1}$  and a G-band at  $1577 \text{ cm}^{-1}$ . The latter corresponded to the first-order scattering of the E<sub>2g</sub> mode. The prominent D peak was due to the structural imperfections in the

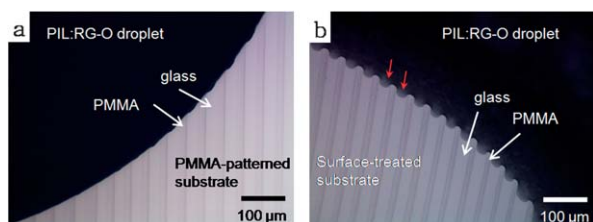


**Fig. 3** Optical micrographs of a drop of the PIL:RG-O suspension spread on the PMMA micro-patterns (a) without surface treatment by O<sub>2</sub> plasma (*i.e.*, as-prepared PMMA stripes used), and (b) with surface treatment by O<sub>2</sub> plasma.

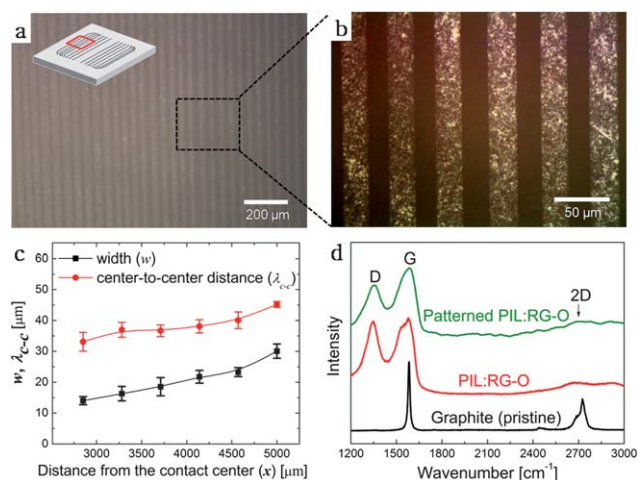


**Fig. 4** (a and b) Optical micrographs of PIL:RG-O micropatterns after the removal of the PMMA template. (c) The width of PIL:RG-O patterns,  $w$ , and the average spacing between adjacent patterns,  $\lambda$ , as a function of  $x$ . (d) Raman spectra of PIL:RG-O patterns (black curve: graphite (*i.e.*, pristine sample); red curve: PIL:RG-O bulk sample; green curve: PIL:RG-O micropatterns prepared using the PMMA template).

RG-O platelets; this is likely related to the presence of residual oxygen and point defects, which is typical for RG-O.

To further scrutinize the surface morphology of the assembled PIL:RG-O platelets, AFM measurements were performed, in which a sharp line width and vertical sidewall were seen (Fig. 5a). The uneven surface of the PIL:RG-O platelets was also observed, which presumably occurred when the PIL:RG-O platelets were pushed into the confined region imposed by the PMMA template during the evaporative assembly process, and thus closely packed together (Fig. 5b and c). The average thickness of the pattern was about 15 nm based on the AFM section analysis, suggesting that the pattern was composed of tens of stacked PIL:RG-O platelets.

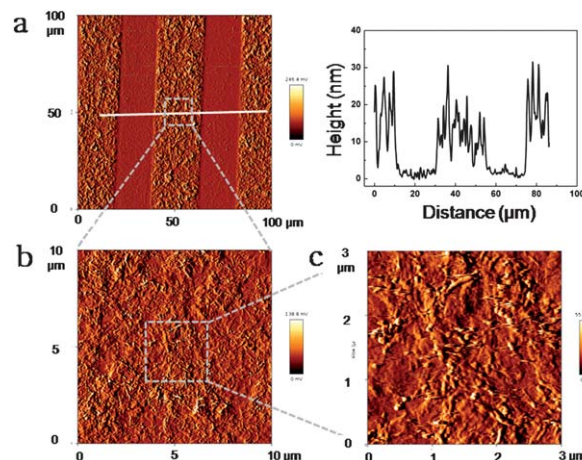


**Fig. 5** AFM phase images of the assembled PIL:RG-O micropatterns. (a) Scan size =  $100 \mu\text{m} \times 100 \mu\text{m}$ ; the section analysis yielded the thickness of the micropattern (right panel). (b) Close-up view of (a); scan size =  $10 \mu\text{m} \times 10 \mu\text{m}$ . (c) Closeup view of (b), in which PIL:RG-O were closely packed; scan size =  $3 \mu\text{m} \times 3 \mu\text{m}$ .

The electrical properties of the PIL:RG-O patterns on the glass substrate were investigated using the two-probe measurements with the silver contacts. The distance between the silver pastes was 4 mm. Fig. 6a shows the  $I$ - $V$  curves of the patterned PIL:RG-O films, which exhibited typical linear ohmic behaviors with a higher surface resistance of 37 M $\Omega$  compared with other literature.<sup>39</sup> The rather high surface resistance of the PIL:RG-O patterns was most likely due to the presence of residual oxygen groups on the basal plane, edges of the RG-O platelets, the PIL coating layer on the RG-O surface and the scattering effects that arose from RG-O stacking. To enhance the electrical properties of the PIL:RG-O patterns, the post-thermal reduction procedure was performed by heating the sample at 300 °C for 20 min. This led to a significant decrease in the resistance by an order of magnitude (2.9 M $\Omega$ ) due to removal of oxygen-based functional groups in PIL:RG-O patterns. Transmission measurements showed that the patterned PIL:RG-O film on the glass substrate had an average of  $\sim$ 90% transmittance in the visible range (Fig. 6b). Taken together, the measured electrical and optical properties of the PIL:RG-O micropatterns suggested that the assembling method described in this study is amenable to the fabrication of graphene-based devices for various applications.

## Experimental section

### Preparation of PIL-modified RG-O (PIL:RG-O) suspension

Graphite oxide (GO) was synthesized using the modified Hummers method,<sup>40</sup> and poly(ionic liquid) (PIL) of poly(1-vinyl-3-ethylimidazolium) bromide was synthesized in accordance with previous reports.<sup>41,42</sup> The dried GO powder (20 mg) was first suspended in deionized water (20 mL) by sonication, followed by the addition of PIL (75 mg). The resulting mixture was further sonicated for 30 min to obtain a fine dispersion of graphene oxide (G-O) modified with PIL. For the chemical reduction, hydrazine monohydrate (0.2 mL) was added to the aqueous dispersion of G-O (1 mg mL<sup>-1</sup>) and PIL in water. The resulting mixture was heated to 90 °C for 1 h. The color of the dispersion changed from yellow-brown to black, indicating the successful reduction of G-O into RG-O, of which the surfaces were coated with PIL. The resultant PIL-modified RG-O (PIL:RG-O) was available as a colloidal system in water.

### Assembly of PIL:RG-O on PMMA pre-patterned substrates

Poly(methyl methacrylate) (PMMA; number-average molecular weight,  $M_n$  = 133 kg mol<sup>-1</sup>, and polydispersity index, PDI = 1.64)

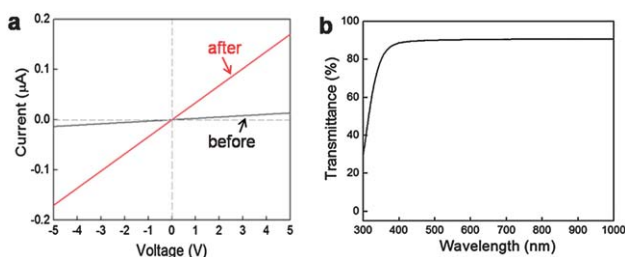


**Fig. 6** (a)  $I$ - $V$  characteristics of patterned PIL:RG-O films before and after post-thermal treatment (black curve: before post-thermal treatment; red curve: after post-thermal treatment). (b) Optical transmittance of PIL:RG-O micropatterns on the glass substrate.

was dissolved in toluene to make the PMMA toluene solution at a concentration of 0.8 mg mL<sup>-1</sup> and then purified with a 0.2  $\mu$ m hydrophobic membrane filter. Glass substrates were cleaned several times in ethanol and dried in an oven. Prior to use, the cleaned substrates were treated with a sulfuric acid solution (Nanostrip 2X, Cyantek corp.) to impart hydrophilicity on the surface. The cylindrical lens and glass substrate were firmly fixed on the top and bottom of the sample holder inside a sealed chamber. After the upper lens was brought into contact with the substrate, a drop of PMMA toluene solution (30  $\mu$ L) was loaded in the cylinder-on-flat geometry composed of the cylindrical lens sitting on the flat glass substrate. After the completion of solvent evaporation at room temperature, concentric rectangle-shaped PMMA patterns were formed on the glass substrate. Locally, they appeared as parallel stripes. The template was then exposed to the O<sub>2</sub> plasma for 20 s at 200 W to promote its surface hydrophilicity. Subsequently, an aqueous PIL:RG-O suspension (40  $\mu$ L) was cast on the PMMA template. After water was completely evaporated, the sample was immersed in toluene to dissolve the PMMA template, followed by mild sonication in ethanol for 60 min. Finally, the sample was dried and the PIL:RG-O micropatterns on the glass substrate were examined by optical microscopy (OM) and atomic force microscopy (AFM).

### Characterizations

$\zeta$  Potential measurements (ELSZ-2, Otsuka electronics) were performed on the PIL-modified RG-O suspension in water. The RG-O patterns were visualized by OM (Leica DMR) in the reflectance mode. The Raman spectra of the PIL:RG-O patterns were obtained with a Raman spectrometer (Jobin-Yvon, LabRam HR) equipped with an Ar-ion laser at 514.5 nm. Surface morphologies of RG-O patterns were obtained by AFM (JPK Instrument, NanoWizard) in tapping mode.  $I$ - $V$  measurements were performed using a two-probe configuration under ambient conditions.

## Conclusions

In summary, we developed an efficient method that is the combination of *controlled evaporative self-assembly (CESA)* and subsequent *directed assembly* to craft highly ordered reduced graphene oxide (RG-O) micro-patterns using the self-assembled polymer template. Central to this strategy is to fabricate the polymer template over large area *via CESA*, and treat the templated glass substrate with the O<sub>2</sub> plasma to render the favorable interaction between the RG-O platelets and the substrate, thereby yielding well-defined microscopic RG-O patterns on the large scale. This simple yet robust, non-lithography method provides a new means of patterning RG-O into microscopic features, which may find potential applications in graphene-based devices.

## Acknowledgements

This work was supported by the Technology Innovation Program, funded by the Ministry of Knowledge Economy (MKE, Korea) and the InsCon Tech, Co. Ltd (Republic of Korea), and the National Science Foundation (NSF CBET-0844084).

## Notes and references

1 A. K. Geim and K. S. Novoselov, *Nat. Mater.*, 2007, **6**, 183.

- 2 D. V. Kosynkin, A. L. Higginbotham, A. Sinitskii, J. R. Lomeda, A. Dimiev, B. K. Price and J. M. Tour, *Nature*, 2009, **458**, 872.
- 3 D. Li and R. B. Kaner, *Science*, 2008, **320**, 1170.
- 4 L. Jiao, L. Zhang, X. Wang, G. Diankov and H. Dai, *Nature*, 2009, **458**, 877.
- 5 X. Li, W. Cai, J. An, S. Kim, J. Nah, D. Yang, R. Piner, A. Velamakanni, I. Jung, E. Tutuc, S. K. Banerjee, L. Colombo and R. S. Ruoff, *Science*, 2009, **324**, 1312.
- 6 K. S. Novoselov, A. K. Geim, S. V. Morozov, D. Jiang, Y. Zhang, S. V. Dubonos, I. V. Grigorieva and A. A. Firsov, *Science*, 2004, **306**, 666.
- 7 S. Park and R. S. Ruoff, *Nat. Nanotechnol.*, 2009, **4**, 217.
- 8 V. C. Tung, M. J. Allen, Y. Yang and R. B. Kaner, *Nat. Nanotechnol.*, 2009, **4**, 25.
- 9 D. R. Dreyer, S. Park, C. W. Bielawski and R. S. Ruoff, *Chem. Soc. Rev.*, 2010, **39**, 228.
- 10 Y. Zhu, S. Murali, W. Cai, X. Li, J. W. Suk, J. R. Potts and R. S. Ruoff, *Adv. Mater.*, 2010, **22**, 3906.
- 11 J. Bai, X. Zhong, S. Jiang, Y. Huang and X. Duan, *Nat. Nanotechnol.*, 2010, **5**, 190.
- 12 S. Pang, H. N. Tsao, X. Feng and K. Müllen, *Adv. Mater.*, 2009, **21**, 3488.
- 13 E. Rabani, D. R. Reichman, P. L. Geissler and L. E. Brus, *Nature*, 2003, **426**, 271.
- 14 T. P. Bigioni, X. M. Lin, T. T. Nguyen, E. I. Corwin, T. A. Witten and H. M. Jaeger, *Nat. Mater.*, 2006, **5**, 265.
- 15 B. P. Khanal and E. R. Zubarev, *Angew. Chem.*, 2007, **119**, 2245.
- 16 Z. Xu and C. Gao, *ACS Nano*, 2011, **5**, 2908.
- 17 Z. Lin, *J. Polym. Sci., Part B: Polym. Phys.*, 2010, **48**, 2552.
- 18 M. Byun, W. Han, N. B. Bowden, F. Qiu and Z. Lin, *Small*, 2010, **6**, 2250.
- 19 M. Byun, R. L. Laskowski, M. He, F. Qui, M. Jeffries-El and Z. Lin, *Soft Matter*, 2009, **5**, 1583.
- 20 M. Byun, N. B. Bowden and Z. Lin, *Nano Lett.*, 2010, **10**, 3111.
- 21 M. Byun, S. W. Hong, F. Qiu, Q. Zou and Z. Lin, *Macromolecules*, 2008, **41**, 9312.
- 22 M. Byun, S. W. Hong, L. Zhu and Z. Lin, *Langmuir*, 2008, **24**, 3525.
- 23 S. W. Hong, J. Xia and Z. Lin, *Adv. Mater.*, 2007, **19**, 1413.
- 24 J. Xu, J. Xia and Z. Lin, *Angew. Chem., Int. Ed.*, 2007, **46**, 1860.
- 25 S. W. Hong, S. Giri, V. S.-Y. Lin and Z. Lin, *Chem. Mater.*, 2006, **18**, 5164.
- 26 S. W. Hong, W. Jeong, H. Ko, M. R. Kessler, V. V. Tsukruk and Z. Lin, *Adv. Funct. Mater.*, 2008, **18**, 2114.
- 27 Z. Lin and S. Granick, *J. Am. Chem. Soc.*, 2005, **127**, 2816.
- 28 J. Xu, J. Xia, S. W. Hong, Z. Lin, F. Qiu and Y. Yang, *Phys. Rev. Lett.*, 2006, **96**, 066104.
- 29 S. W. Hong, M. Byun and Z. Lin, *Angew. Chem., Int. Ed.*, 2009, **48**, 512.
- 30 S. W. Hong, J. Xu and Z. Lin, *Nano Lett.*, 2006, **6**, 2949.
- 31 S. W. Hong, J. Xia, M. Byun, Q. Zou and Z. Lin, *Macromolecules*, 2007, **40**, 2831.
- 32 S. W. Hong, J. Xu, J. Xia, Z. Lin, F. Qiu and Y. Yang, *Chem. Mater.*, 2005, **17**, 6223.
- 33 D. A. Dikin, S. Stankovich, E. J. Zimney, R. D. Piner, G. H. B. Dommett, G. Evmenenko, S. T. Nguyen and R. S. Ruoff, *Nature*, 2007, **448**, 457.
- 34 G. Eda, G. Fanchini and M. Chhowalla, *Nat. Nanotechnol.*, 2008, **3**, 270.
- 35 G. Eda and M. Chhowalla, *Adv. Mater.*, 2010, **22**, 2392.
- 36 T. Kim, H. Lee, J. Kim and K. S. Suh, *ACS Nano*, 2010, **4**, 1612.
- 37 R. D. Deegan, O. Bakajin, T. F. Dupont, G. Huber, S. R. Nagel and T. A. Witten, *Nature*, 1997, **389**, 827.
- 38 R. D. Deegan, O. Bakajin, T. F. Dupont, G. Huber, S. R. Nagel and T. A. Witten, *Phys. Rev. E: Stat. Phys., Plasmas, Fluids, Relat. Interdiscip. Top.*, 2000, **62**, 756.
- 39 G. Eda, G. Fanchini and M. Chhowalla, *Nat. Nanotechnol.*, 2008, **3**, 270.
- 40 W. S. Hummers and R. E. Offerman, *J. Am. Chem. Soc.*, 1958, **80**, 1339.
- 41 C. Pozo-Gonzalo, R. Marcilla, M. Salsamendi, D. Mecerreyes, J. A. Pomposo, J. Rodriguez and H. J. Bolink, *J. Polym. Sci., Part A: Polym. Chem.*, 2008, **46**, 3150.
- 42 T. Y. Kim, T. H. Lee, J. E. Kim, R. M. Kasi, C. S. P. Sung and K. S. Suh, *J. Polym. Sci., Part A: Polym. Chem.*, 2008, **46**, 6872.